

GATING CURRENT MODELS COMPUTED WITH CONSISTENT INTERACTIONS

Tzyy-Leng Horng¹, Robert S. Eisenberg², Chun
Liu³, Francisco Bezanilla⁴

¹Feng Chia Univ, Taichung, Taiwan, ² Rush Univ., Chicago, IL, USA, ³Penn
State Univ., State College, PA, USA, ⁴Univ. Of Chicago, Chicago, IL, USA

ABSTRACT

Gating currents of the voltage sensor involve back-and forth movements of positively charged arginines through the hydrophobic plug of the gating pore. Transient movements of the permanent charge of the arginines induce structural changes and polarization charge nearby. The moving permanent charge induces current flow everywhere. Everything interacts with everything else in this structural model so everything must interact with everything else in the mathematics, as everything does in the structure. Energy variational methods *EnVarA* are used to compute gating currents in which all movements of charge and mass satisfy conservation laws of current and mass. Conservation laws are partial differential equations in space and time. Ordinary differential equations cannot capture such interactions with one set of parameters. Indeed, they may inadvertently violate conservation of current. Conservation of current is particularly important since small violations (<0.01%) quickly (microseconds) produce forces that destroy molecules. Our model reproduces signature properties of gating current: (1) equality of ON and OFF charge (2) saturating voltage dependence and (3) many (but not all) details of the shape of charge movement as a function of voltage, time, and solution composition. The model computes gating current flowing in the baths produced by arginines moving in the voltage sensor. The movement of arginines induces current flow everywhere producing 'capacitive' pile ups at the ends of the channel. Such pile-ups at charged interfaces are well studied in measurements and theories of physical chemistry but they are not typically included in models of gating current or ion channels. The pile-ups of charge change local electric fields, and they store charge in series with the charge storage of the arginines of the voltage sensor. Implications are being investigated.

INTRODUCTION

Voltage Sensors

Much of biology depends on the voltage across cell membranes. The voltage across the membrane must be sensed before it can be used by proteins. Permanent charges move in the strong electric fields within membranes, so carriers of gating and sensing charge were proposed as voltage sensors even before membrane proteins were known to span lipid membranes (1). Movement of permanent charges of the voltage sensor is **gating current** and movement is the voltage sensing mechanism.

Measurements

Measurement of gating currents is possible because Maxwell's equations guarantee conservation of current. 'Current' is defined in Maxwell's equations as that which produces (the curl of) the magnetic field, that is, the flux of charge plus the 'displacement term' which is ϵ_0 times the rate of change of the electric field. Measurements of gating current were greatly aided by biological preparations with much higher densities of voltage sensors, in which the non-gating currents are a much smaller part of the displacement current.

Structure and sensors

Knowledge of membrane protein structure has allowed us to identify and look at the atoms that make up the voltage sensor. Protein structures do not include the membrane potentials and macroscopic concentrations that power gating currents, therefore simulations are needed.

Atomic level simulations

Molecular (really atomic) dynamics do not provide an easy extension from the atomic time scale 2×10^{-16} sec to the biological time scale of gating currents that reaches 50×10^{-3} sec. Calculations of gating currents from simulations must average the trajectories (lasting 50×10^{-3} sec sampled every 2×10^{-16} sec) of $\sim 10^6$ atoms all of which interact through the electric field to conserve charge and current, while conserving mass. It is difficult to enforce continuity of current flow in simulations of atomic dynamics because simulations compute only local behavior while continuity of current is global, involving current flow far from the atoms that control the local behavior.

Our Modeling Approach

A hybrid approach is needed, starting with the essential knowledge of structure, but computing only those parts of the structure used by biology to sense voltage. In close packed ('condensed') systems like the voltage sensor, or ionic solutions, '*everything interacts with everything else*' because electric fields are long ranged as well as strong. In ionic solutions, ion channels, even in enzyme active sites, steric interactions are also of great importance that prevent the overfilling of space. Closely packed charged systems are best handled mathematically by variational methods. Variational methods guarantee that all variables satisfy all equations (and boundary conditions) at all times and under all conditions

We have then used the energy variational approach developed by Chun Liu (2,3), to derive a consistent model of gating charge movement, based on the basic features of the structure of crystallized channels and voltage sensors. The schematic of the model is shown below.

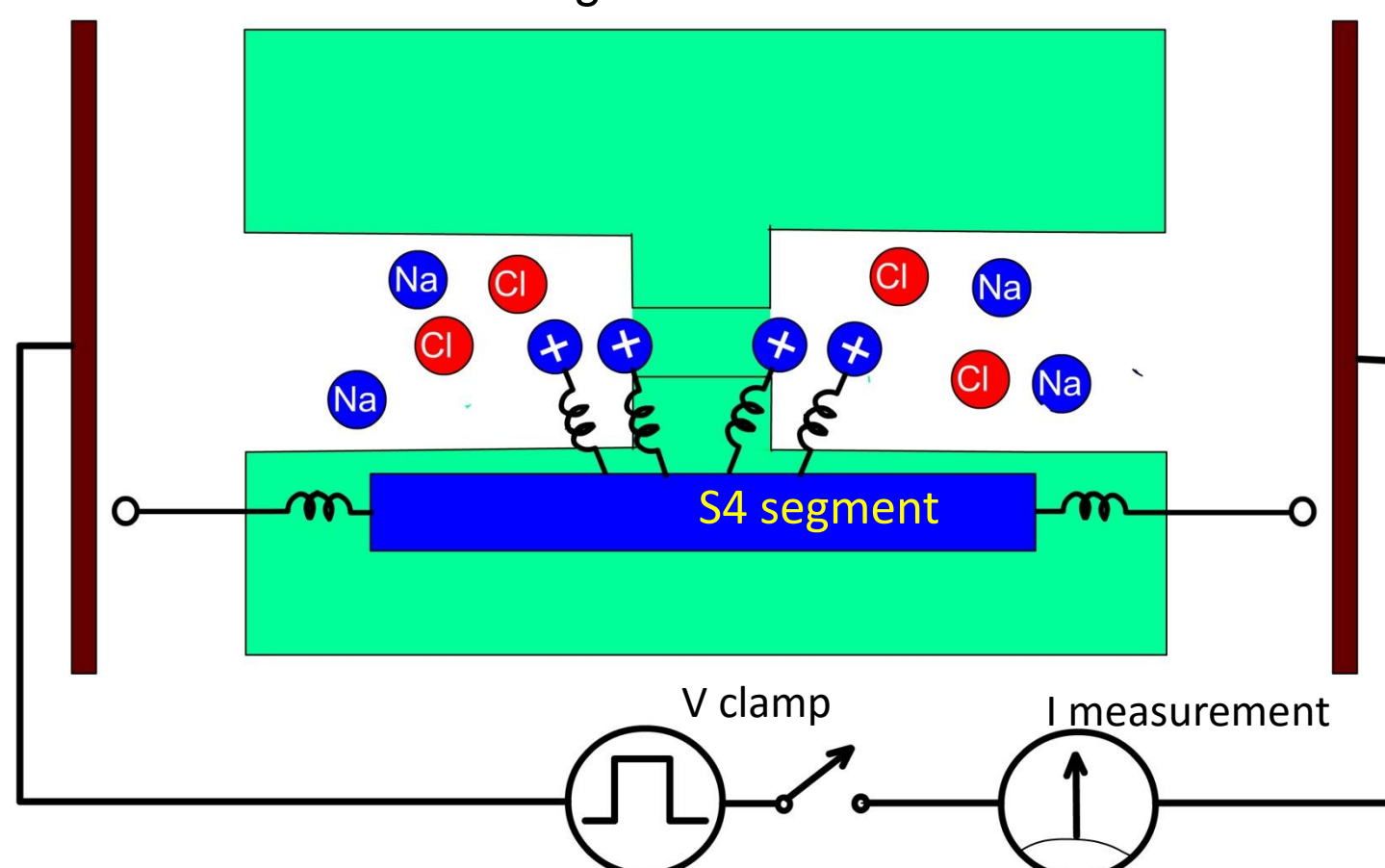


Figure 1. Geometric configuration of the model including the attachments of arginines to the S4 segment

Mathematical Description

The axisymmetric geometric configuration is shown in Fig. 2, with $\Omega_R = [0, L_R] \cup [L + L_R, L + 2L_R]$ (zone 1 and 3) being the antechambers and $\Omega_a = [L_R, L_R + L]$ (zone 2) being the channel. Na and Cl only reside at antechambers and can not enter channel, while 4 arginines (marked 1-4) can reside at both antechambers and channel but can not further exit to the reservoirs outside.

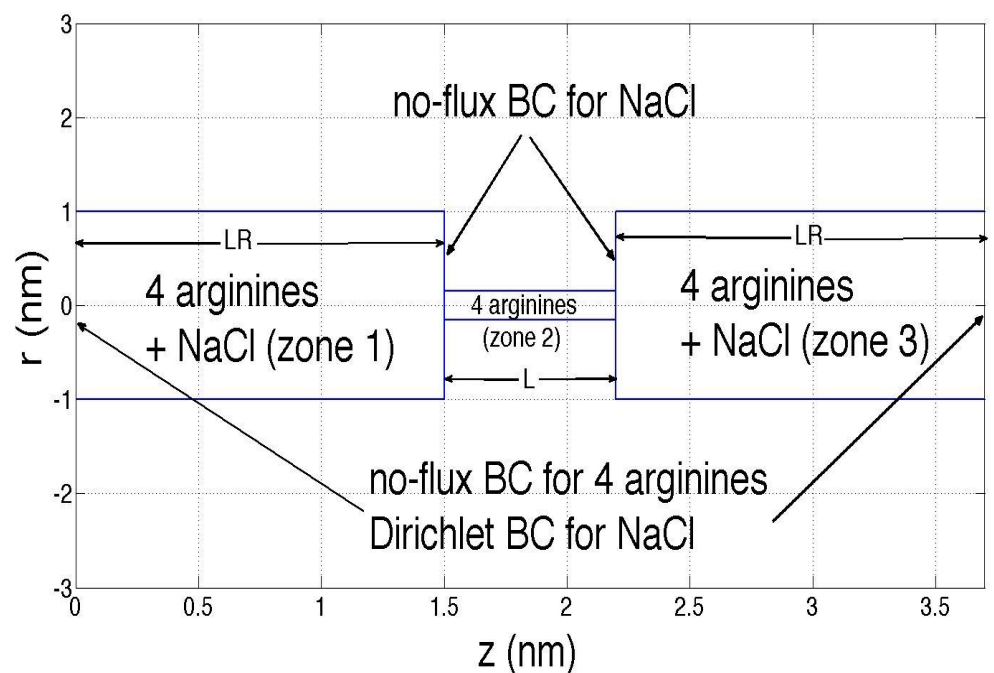


Figure 2. Geometric Configuration for mathematical model.

The reduced 1D dimensionless PNP-steric equations are expressed as below. The first one is Poisson equation:

$$-\frac{1}{A} \frac{d}{dz} \left(\Gamma A \frac{d\phi}{dz} \right) = \sum_{i=1}^N z_i c_i, \quad i = \text{arginines.}, \text{Na, Cl}, \quad (1)$$

with $\Gamma = \frac{\lambda_D^2}{L_{ref}^2}$, $\lambda_D = \sqrt{\frac{\epsilon k_B T}{c_0 e^2}}$ and $A(z)$ being the cross-sectional area. To be specific,

$$A(z) = \pi r_a^2, \quad z \in \Omega_a; \quad A(z) = \pi r_R^2, \quad z \in \Omega_R.$$

$L_{ref}=1\text{nm}$ is the characteristic length here. r_a and r_R are radius of zone 2 and zone 1, 3 respectively. As to valence (charge) of ions $z_{Na} = 1$, $z_{Cl} = -1$. z_{arg} depends on pKa of channel environment, and will be a free parameter to input. The second equation is the transport equation based on conservation law:

$$\frac{\partial c_i}{\partial t} + \frac{1}{A} \frac{\partial}{\partial z} (A J_i) = 0, \quad i = \text{arginines, Na, Cl}. \quad (2)$$

with the content of J_i based on Nernst-Planck equation:

$$J_i = -D_i \left(\frac{\partial c_i}{\partial z} + c_i z_i \frac{\partial \phi}{\partial z} \right), \quad i = \text{Na, Cl}, \quad z \in \Omega_R, \quad (3)$$

and for 4 arginines c_i , $i=1, 2, 3$ and 4, $z \in \Omega_a \cup \Omega_R$,

$$J_1 = -D_1(z) \left(\frac{\partial c_1}{\partial z} + z_{arg} c_1 \frac{\partial \phi}{\partial z} + C_1 \left(\frac{\partial V_1}{\partial z} + \frac{\partial V}{\partial z} \right) + g C_1 \left(\frac{\partial c_2}{\partial z} + \frac{\partial c_3}{\partial z} + \frac{\partial c_4}{\partial z} \right) \right), \quad (4)$$

$$J_2 = -D_2(z) \left(\frac{\partial c_2}{\partial z} + z_{arg} c_2 \frac{\partial \phi}{\partial z} + C_2 \left(\frac{\partial V_2}{\partial z} + \frac{\partial V}{\partial z} \right) + g C_2 \left(\frac{\partial c_1}{\partial z} + \frac{\partial c_3}{\partial z} + \frac{\partial c_4}{\partial z} \right) \right), \quad (5)$$

$$J_3 = -D_3(z) \left(\frac{\partial c_3}{\partial z} + z_{arg} c_3 \frac{\partial \phi}{\partial z} + C_3 \left(\frac{\partial V_3}{\partial z} + \frac{\partial V}{\partial z} \right) + g C_3 \left(\frac{\partial c_1}{\partial z} + \frac{\partial c_2}{\partial z} + \frac{\partial c_4}{\partial z} \right) \right), \quad (6)$$

$$J_4 = -D_4(z) \left(\frac{\partial c_4}{\partial z} + z_{arg} c_4 \frac{\partial \phi}{\partial z} + C_4 \left(\frac{\partial V_4}{\partial z} + \frac{\partial V}{\partial z} \right) + g C_4 \left(\frac{\partial c_1}{\partial z} + \frac{\partial c_2}{\partial z} + \frac{\partial c_3}{\partial z} \right) \right), \quad (7)$$

where D_i , $i=\text{Na, Cl, 1, 2, 3, and 4}$ are diffusion coefficients, and g is the parameter characterizing steric effect. Larger g implies larger steric effect, but g can not be arbitrarily large due to the limitation of stability. V_i , $i=1, 2, 3$ and 4 being the trap potential for c_i

representing a spring connecting c_i to the S4 segment (see Fig. 1). Specifically,

$$V_i(z, t) = K(z - (z_i + \Delta Z_{S4}(t)))^2, \quad (8)$$

where K is the spring constant, z_i is the anchoring position of spring for c_i on S4, $\Delta Z_{S4}(t)$ is the z-direction displacement of S4 by treating S4 as a rigid body. $\Delta Z_{S4}(t)$ follows the motion of equation of S4 based on spring-mass system:

$$m_{S4} \frac{d^2 \Delta Z_{S4}}{dt^2} + b_{S4} \frac{d \Delta Z_{S4}}{dt} + K_{S4} \Delta Z_{S4} = \sum_{i=1}^4 K(z_{i,CM} - z_i), \quad (9)$$

where m_{S4} , b_{S4} and K_{S4} are mass, damping coefficient and restraining spring constant for S4. $z_{i,CM}$ is the center of mass for c_i , which is calculated by

$$z_{i,CM} = \frac{\int_{\Omega_a \cup \Omega_R} A(z) z c_i dz}{\int_{\Omega_a \cup \Omega_R} A(z) c_i dz}, \quad i=1, 2, 3, 4. \quad (10)$$

Usually (9) is over-damped, therefore the inertia term in (9) can then be neglected. The additional potential V in (4-7) is caused by the hydrophobic environment of channel. It can be seen as the solvation energy barrier. If we use Born model to estimate the solvation energy $\Delta E_{solvation}$,

$$\Delta E_{solvation} = \frac{z_{arg}^2 e^2}{8\pi\epsilon_0 r_{arg}} \left(\frac{1}{\epsilon_a} - \frac{1}{\epsilon_R} \right), \quad (11)$$

where ϵ_R and ϵ_a are dielectric constants for antechamber and channel, respectively.

Usually we treat $\epsilon_R = 80$, and then $\epsilon_a = 8$ (here we set $\Gamma = \begin{cases} 1, & z \in \Omega_R, \\ 0.1, & z \in \Omega_a. \end{cases}$). The apparent radius of the guanidinium ion, which is the ionic part of the arginine, is 0.21 nm. With $z_{arg}=1$, we can therefore obtain $\Delta E_{solvation}$ to be close to $15k_B T$.

Here, we set

$$V = V_{max} \left(\tanh(5(z - L_R)) - \tanh(5(z - L - L_R)) - 1 \right), \quad z \in \Omega_a, \quad (12)$$

with V_{max} being the free parameter to input and related to $\Delta E_{solvation}$. Note that tanh function is employed to smooth the top-hat-shape barrier profile, which is not good for differentiation.

Boundary and interface conditions for electric potential ϕ are

$$\begin{aligned} \phi(0) &= \phi_L, & \phi(L_R^-) &= \phi(L_R^+), & \Gamma(L_R^-)A(L_R^-) \frac{d\phi}{dz}(L_R^-) &= \Gamma(L_R^+)A(L_R^+) \frac{d\phi}{dz}(L_R^+), \\ \phi(L_R + L^-) &= \phi(L_R + L^+), \\ \Gamma(L_R + L^-)A(L_R + L^-) \frac{d\phi}{dz}(L_R + L^-) &= \Gamma(L_R + L^+)A(L_R + L^+) \frac{d\phi}{dz}(L_R + L^+), \\ \phi(2L_R + L) &= 0. \end{aligned} \quad (13)$$

Boundary and interface conditions for arginine are

$$\begin{aligned} J_i(0, t) &= J_i(2L_R + L, t) = 0, & c_i(L_R^+, t) &= c_i(L_R^-, t), & J_i(L_R^-, t) &= J_i(L_R^+, t), \\ c_i(L_R + L^-, t) &= c_i(L_R + L^+, t), & J_i(L_R + L^-, t) &= J_i(L_R + L^+, t), & i &= 1, 2, 3, 4. \end{aligned} \quad (14)$$

Boundary conditions for Na and Cl are

$$\begin{aligned} c_{Na}(0, t) &= c_{Cl}(0, t) = c_{Na}(2L_R + L, t) = c_{Cl}(2L_R + L, t) = 1, \\ J_{Na}(L_R, t) &= J_{Cl}(L_R, t) = J_{Na}(L_R + L, t) = J_{Cl}(L_R + L, t) = 0. \end{aligned} \quad (15)$$

Initial conditions are

$$c_{Na}(z, 0) = c_{Cl}(z, 0) = 1, \quad z \in \Omega_R; \quad c_i(z, 0) = Q, \quad z \in \Omega_a \cup \Omega_R, i = 1, 2, 3, 4. \quad (16)$$

Input parameter and its value: $L_R=1.5, L=0.7, r_a=0.15, r_R=1, z_{arg}=1, D_i(z)=D_{arg}=5, i=1, 2, 3, 4, Q=0.1, g=0.5, V_{max}=5, K=3, K_{S4}=12, b_{S4}=6.$

The most important parameter to be varied for investigation is ϕ_L . Note that ϕ_L is dimensionless. Changing to a dimensional one will be multiplied by 25mV.

Outputs: gating current I at $z=L_R+L/2$; $Q_1 = \frac{\int_0^{L_R} A(z) \sum_{i=1}^4 c_i dz}{\int_0^{2L_R+L} A(z) \sum_{i=1}^4 c_i dz}, \quad Q_2 = \frac{\int_{L_R}^{L_R+L} A(z) \sum_{i=1}^4 c_i dz}{\int_0^{2L_R+L} A(z) \sum_{i=1}^4 c_i dz},$

$Q_3 = \frac{\int_{L_R+L}^{2L_R+L} A(z) \sum_{i=1}^4 c_i dz}{\int_0^{2L_R+L} A(z) \sum_{i=1}^4 c_i dz}$ are volume fraction of arginine in zone 1, 2 and 3, respectively.

$z_{i,CM}(t)$ and time course of gating charge (time integral of gating current at $z=L_R+L/2$) are also outputs to be compared.

Numerical Methods

High-order multi-block Chebyshev pseudospectral methods are used here to discretize (1) and (2) in space. The resultant semi-discrete system is then a set of coupled ordinary differential equations in time, chiefly from (2), and algebraic equations, chiefly from (1) and boundary/interface conditions (13-15). This system is further integrated in time by an ODAE solver (ODE15S in MATLAB) together with the initial condition (16). High-order pseudospectral methods provides good accuracy with economic resolutions. ODE15S is a variable-order-variable-step (VSVO) solver, which is highly efficient in time integration. With these two highly efficient techniques, we can conduct fast simulations to find results comparable with experiments through tuning a large set of parameters.

Note on units: time (t) is dimensionless and is normalized by L^2/D_{ref} , $D_{ref}=D_{arg}/5$ here
distance (z) is in nanometers

RESULTS

We explored several parameter values to obtain charge movement with kinetics and steady state properties similar to the experimentally recorded gating currents. Parameters selected were: $L=0.7, K=3, K_s=12, b=6$, distance between arginines= 0.4 nm.

Time course of Gating current and total Arginine movement

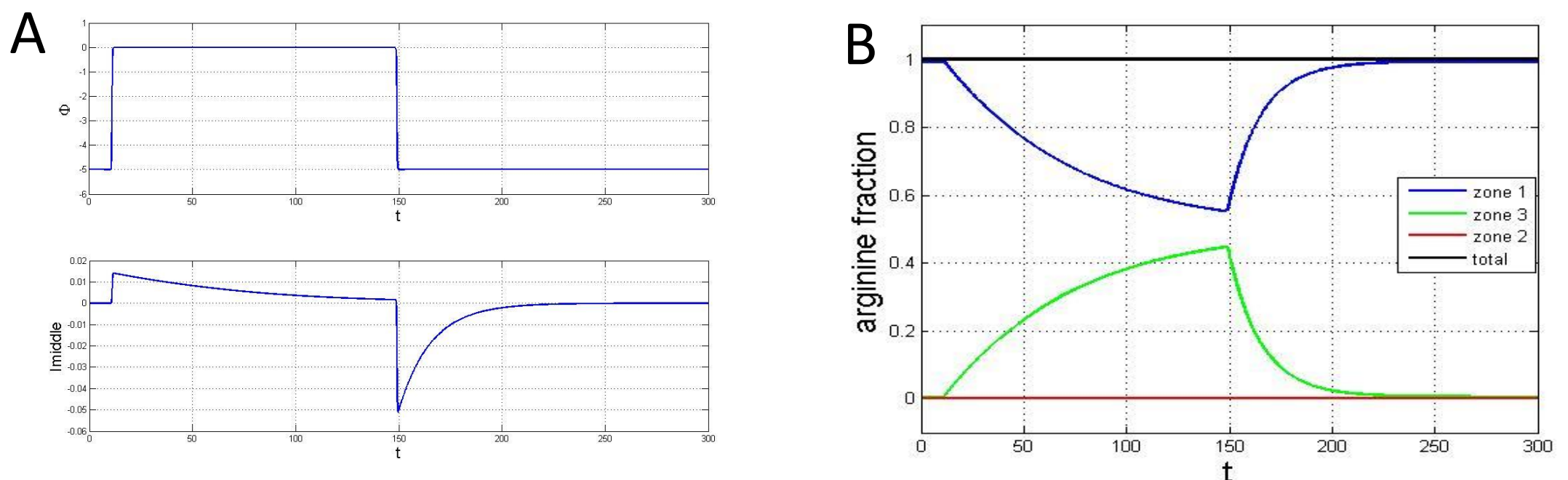


Figure 3. A. Example of gating current obtained by pulsing from -125 to 0 mV. **B.** Time course of arginines volume fraction in the three compartments of the sensor

Time course of arginine translocation and voltage profile

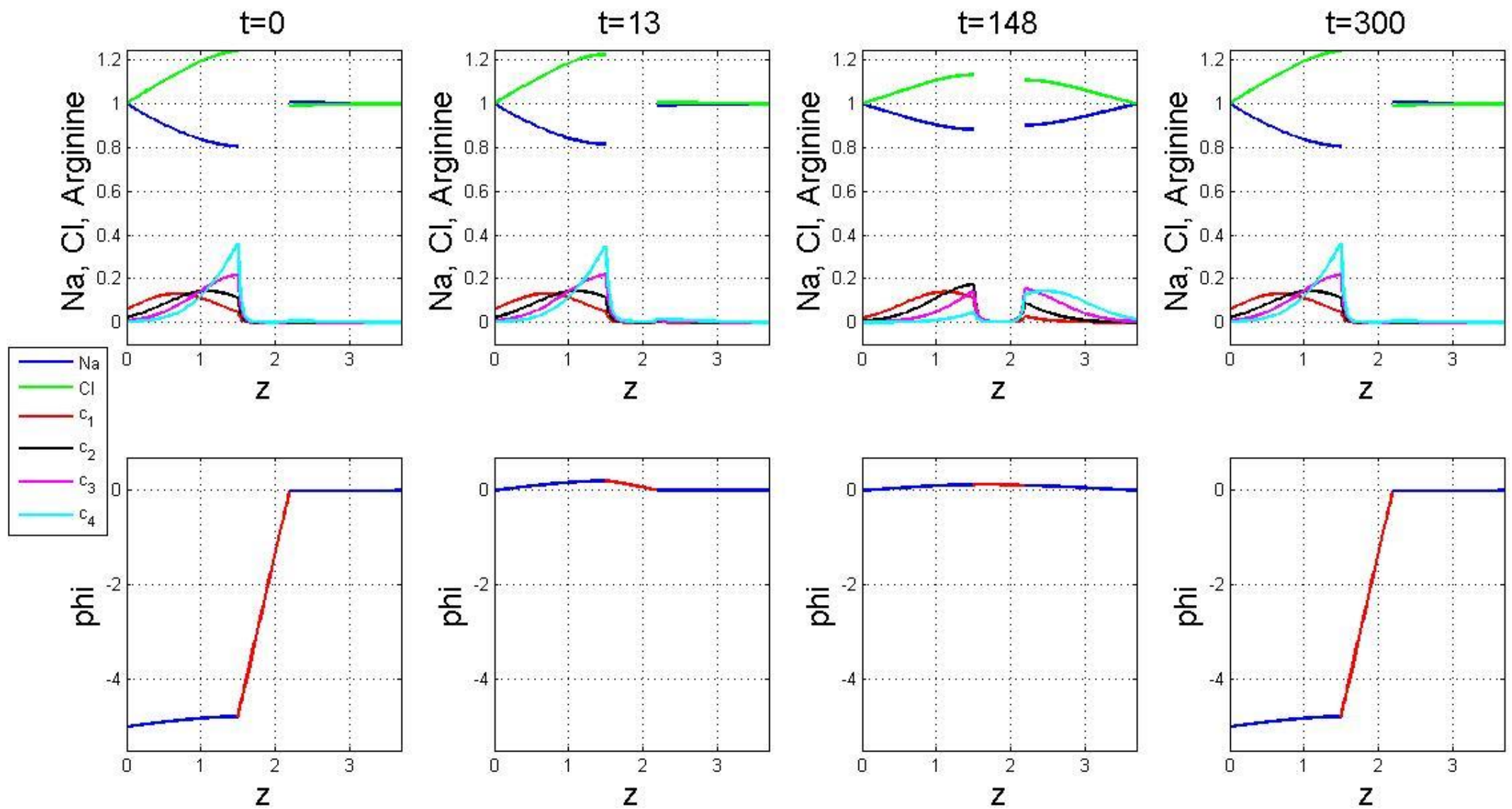


Figure 4. The four panels on the **top row** show how the individual arginines distribute in the different regions of the sensor depending on voltage and time (as indicated at the top) as a result of a pulse to 0 mV starting at $t=10$ and ending at $t=150$. The relative concentration of ions, Na (blue) and Cl (green) change in the vestibules to compensate for the charge of the arginines present in the vestibule. Arginines are color coded starting from the left c_1 (red), c_2 (black), c_3 (magenta) and c_4 (cyan). Note that the concentration of arginines in the channel is close to zero at all times. The four panels on the **bottom row** show the potential profile in the voltage sensor at different times (as indicated at the top). By definition, the right side is always maintained at 0 mV. By comparing the profile at $t=13$ and $t=148$ is clear that the potential profile changes as the arginines move from left to right even though the voltage is maintained constant across the sensor.

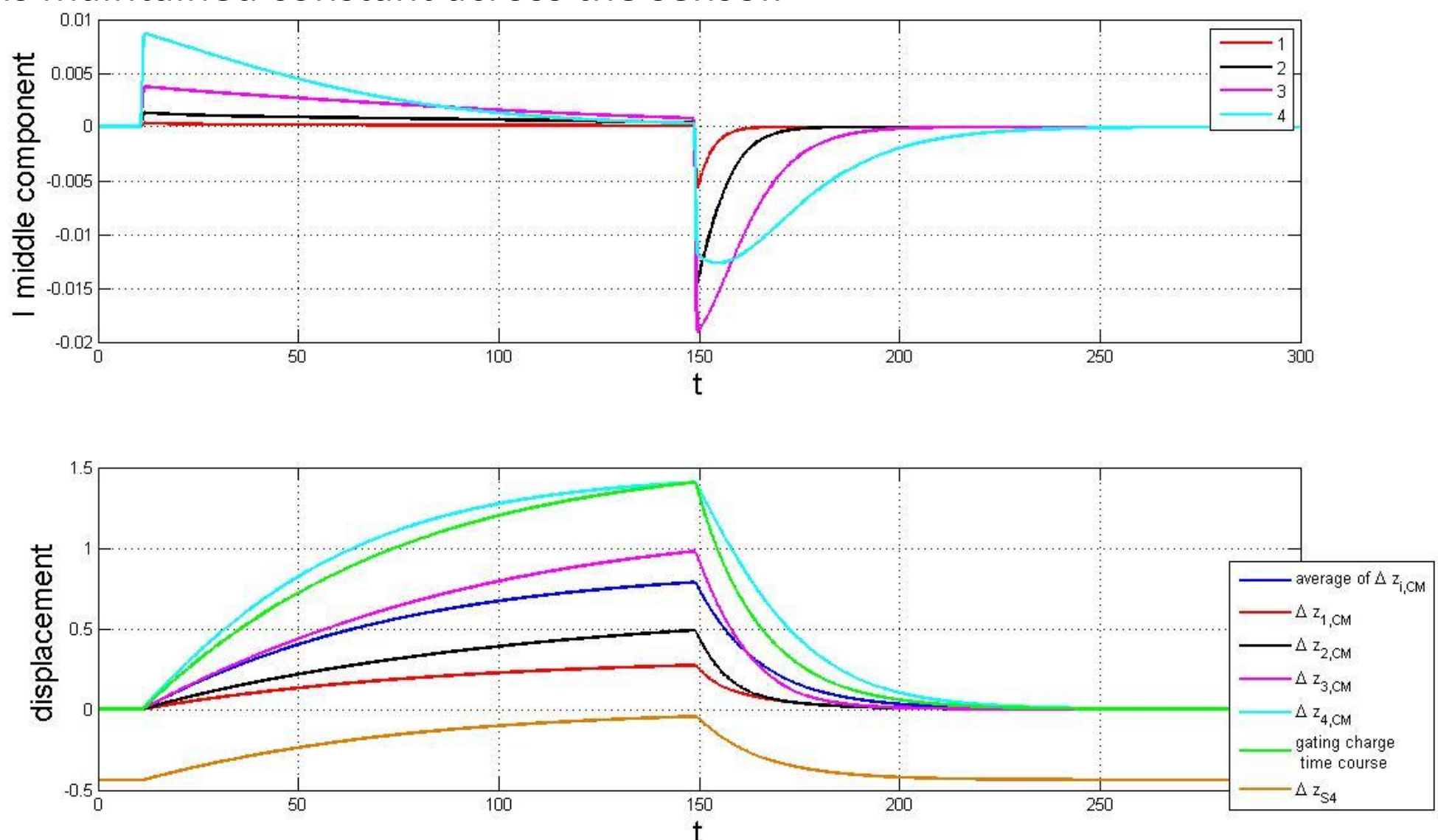


Figure 5. Top Panel. Time course of gating current contribution of individual arginines. **Bottom Panel,** displacement of individual arginines center of mass ($\Delta z_{i,CM}, i=1\dots 4$) compared to gating charge (green) and displacement of S4 segment center of mass Δz_{S4} .

Large depolarization (to saturating voltage)

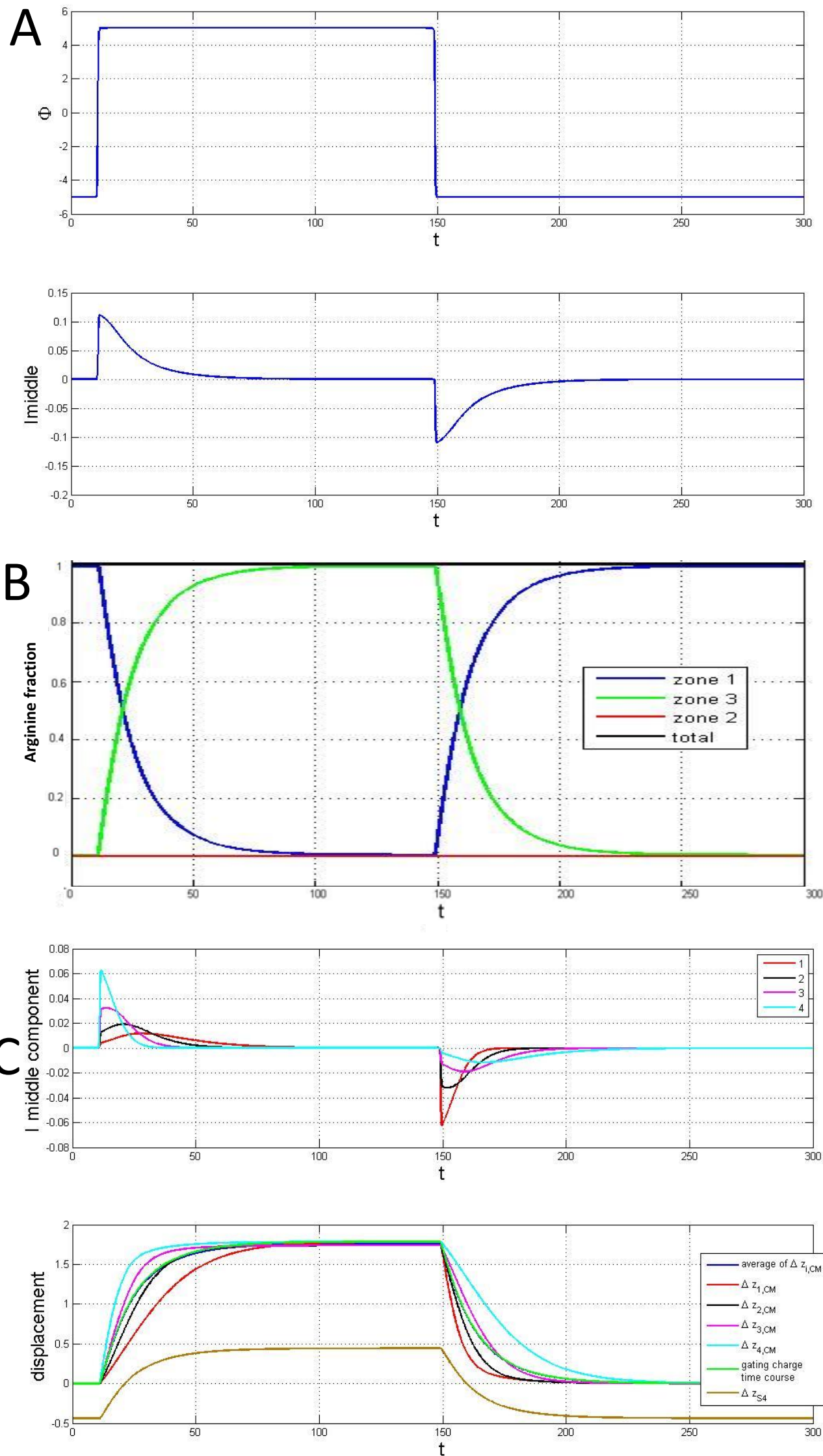


Figure 6. A. Time course of gating current for a pulse to 125 mV from a holding of -125 mV, showing the total charge movement. Note that the kinetics of the decay of gating current at this potential is much faster than the decay at 0 mV, shown in Figure 1. However the off time course in both cases are similar.

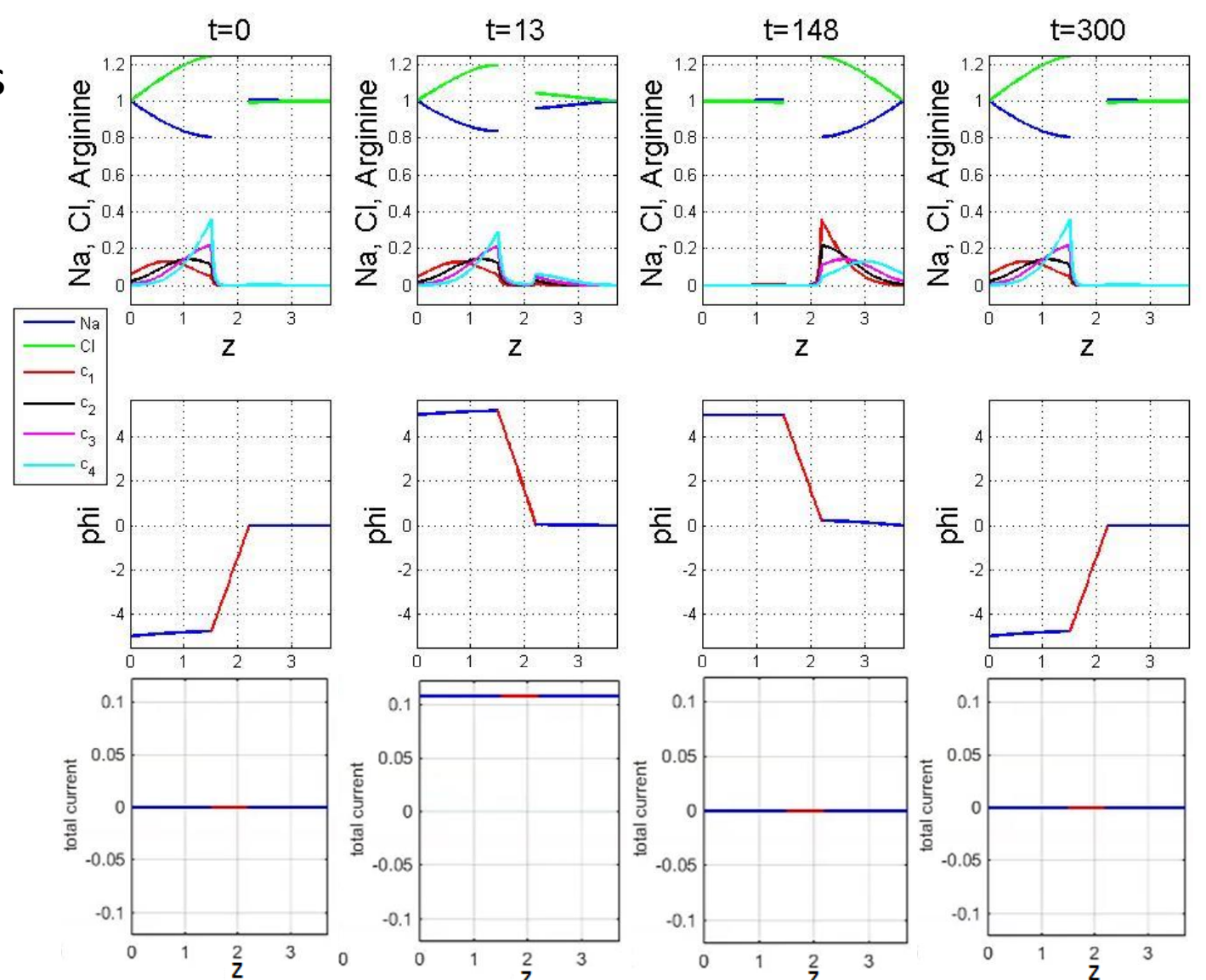
B. Time course of arginine fraction in the three compartments of the sensor. Note that at this voltage most of the arginines have been translocated and the concentration in the channel is zero.

C. Top Panel. Time course of the contribution of each arginine to the gating current. **Bottom panel,** displacement of individual arginines center of mass ($\Delta z_{i,CM}, i=1...4$) compared to gating charge (green) and displacement of S4 segment (Δz_{S4} , brown). Notice that the S4 segment moves a total of 0.88 nm (8.8 Å) while individual arginines move as much as 1.5 nm, showing that the side chain movement contributes significantly to the total movement of the charged residues.

Figure 7. Top row shows distribution of individual arginines as a function of distance at different times for a pulse to 125 mV. Conventions as in Figure 4.

Middle row shows the potential profile as a function of distance in the voltage sensor at different times for a pulse to 125 mV. Conventions as in Figure 4.

Bottom Row shows the current profile as a function of distance. Notice that the model satisfies conservation of current at all times.



Family of gating currents for a range of voltages

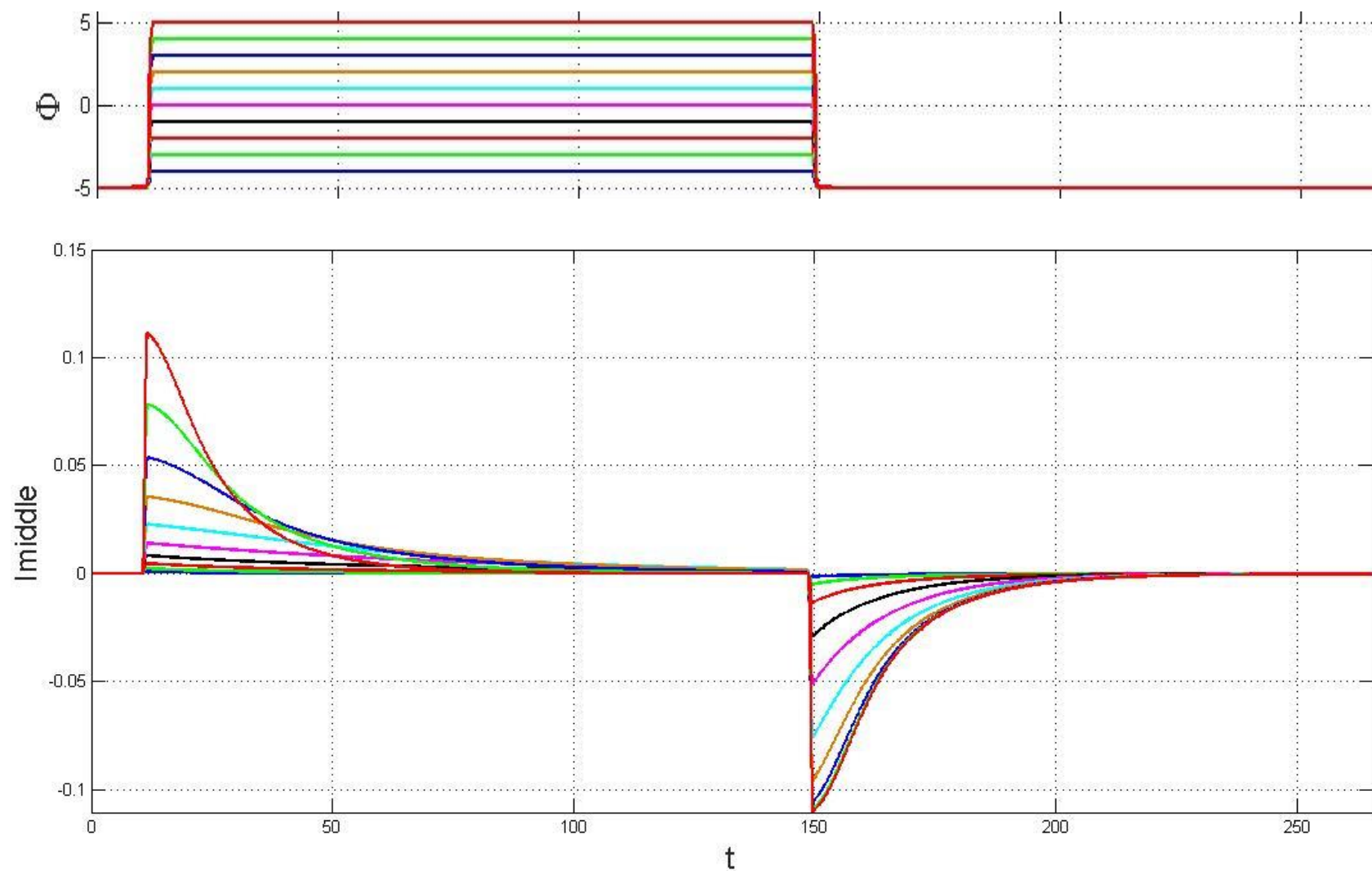


Figure 8. I-V curve. Top panel. Voltage pulses (holding: -125 mV, pulse to 125 mV every 25 mV). Bottom panel. Gating currents for pulses indicated in left panel. Note that the current at large potentials cross the current at small voltages showing that kinetics is voltage dependent.

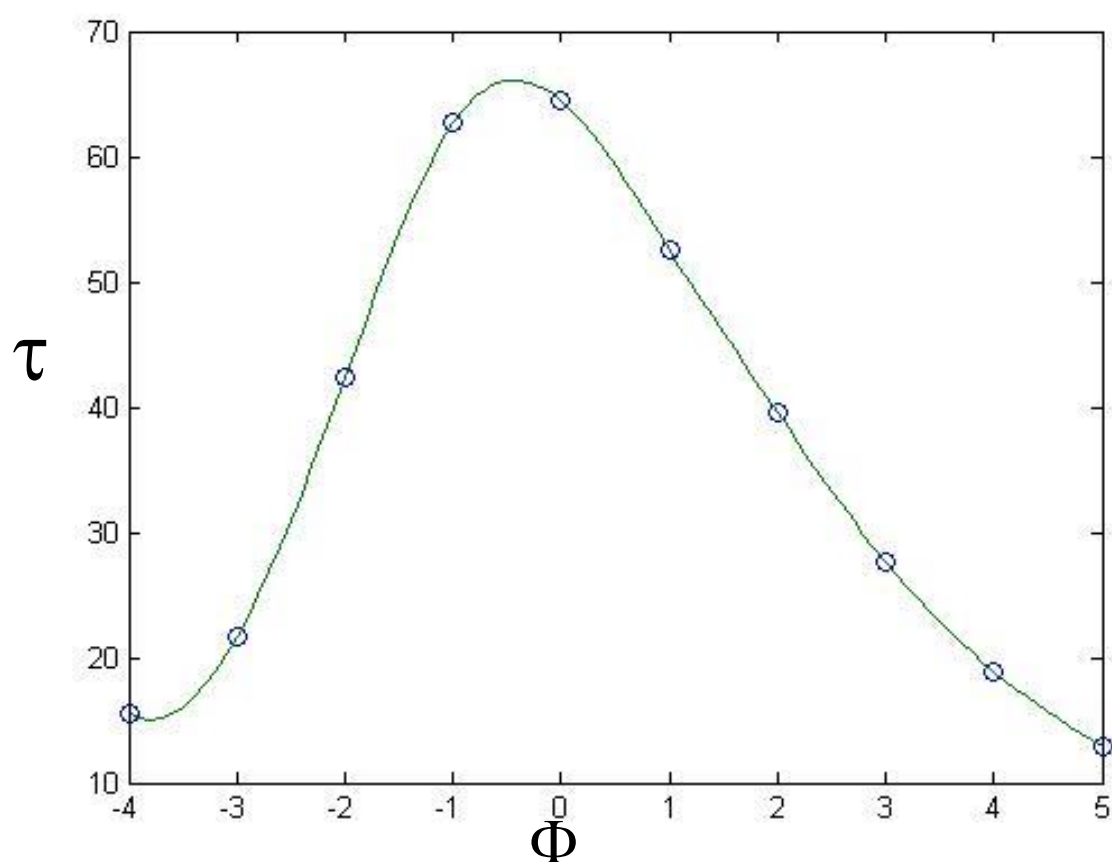


Figure 9. Kinetics. The voltage dependence of the gating current decay is bell-shaped as seen experimentally. Gating currents of Figure 6 were fit with to $ae^{-t/\tau_1} + be^{-t/\tau_2}$ after the peak and the weighted average τ was plotted as a function of the voltage of the pulse.

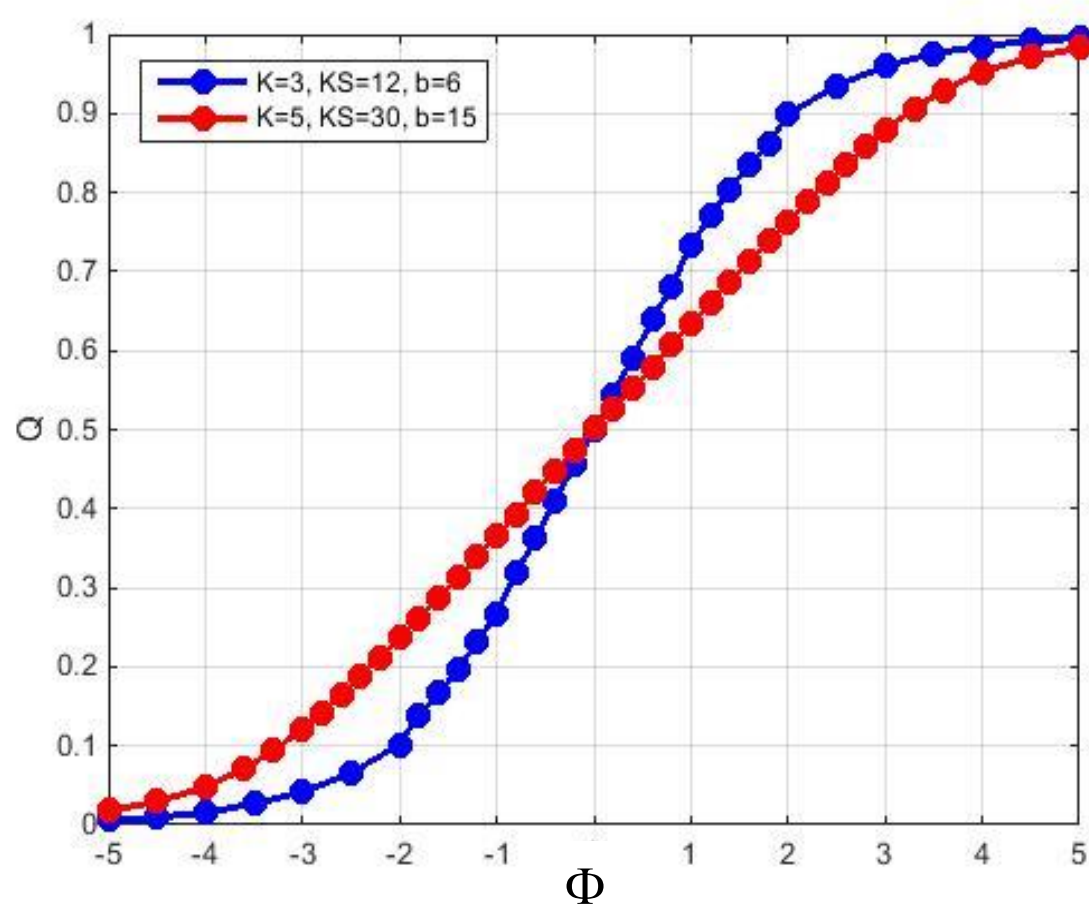


Figure 10. Steady-state. The voltage dependence of the charge transferred (Q-V curve) is sigmoidal as seen experimentally. The blue curve corresponds to the parameters used in all the graphs shown. The red curve shows a Q-V curve with increased values of the spring constants of the arginine and the S4, as well as the friction of the S4, demonstrating that these parameters determine the steepness of the gating charge voltage dependence. The midpoint of the Q-V is at 0 mV because we have not biased the S4 position.

DISCUSSION AND PERSPECTIVE

- The present model of the voltage sensor is an attempt at capturing the essential structural details that are necessary to reproduce the basic features of experimentally recorded gating currents. After finding appropriate parameters, we found that the general kinetic and steady-state properties are well represented by the simulations. This indicates that this approach, which takes in account all interactions, and satisfies conservation of current, is a good model of voltage sensors.
- There are some differences between the predictions of the model and the experiments, most notably that the Q-V curve predicted is less steep than the experimental one, even after decreasing the spring constants significantly (see Fig. 8). This may reveal an important limitation in the present formulation, that is, the fact that arginines may move more cooperatively cross the channel.
- The present dielectric energy term in the channel is an approximation of the Born potential and at present has been left fixed. This is probably the weakest point in this model because it oversimplifies the interactions of the channel dielectric with the arginines as they move through the channel.
- The next step is to model the details of interactions of the moving arginines with the wall of the channel. There is plenty of detailed information on the amino acid side chains in the channel and how each one of them have important effects in the kinetics and steady-state properties of gating charge movement (4). The studied side chains reveal steric as well as dielectric interactions with the arginines that the present model does not have. On the other hand, the power of the present mathematical modeling is precisely the implementation of interactions, therefore we believe that when we add the dielectric details of the channel a better prediction of the currents should be attained and it is even possible that the cooperativity between arginines may occur.
- Further work must address the mechanism of coupling between the voltage sensor movements and the conduction pore. It seems likely that the classical mechanical models will need to be extended to include coupling through the electrical field. It is possible that the voltage sensor modifies the stability of conduction current.

REFERENCES

1. Hodgkin, A.L. and Huxley, A.F. (1952) "A quantitative description of membrane current and its application to conduction and excitation in nerve". *J. Physiol.* 117:500-544.
2. Eisenberg, B., et al. (2010). "Energy Variational Analysis EnVarA of Ions in Water and Channels: Field Theory for Primitive Models of Complex Ionic Fluids." *Journal of Chemical Physics* 133: 104104
3. Horng, T.-L., et al. (2012). "PNP Equations with Steric Effects: A Model of Ion Flow through Channels." *The Journal of Physical Chemistry B* 116(37): 11422-11441.
4. Lacroix, J. J., Hyde, H.C., Campos, F.V., and Bezanilla, F. (2014) "Moving gating charges through the gating pore in a Kv channel voltage sensor" *PNAS* 119:E1950-E1959.